

The influence of stellar wind bubbles on the ionizing radiation field in HII regions

*I. O. Koshmak**, *B. Ya. Melekh†*

Ivan Franko National University of Lviv, Kyryla i Mefodia str., 8, 79005, Lviv, Ukraine

Stellar wind around starbursts forms cavities filled by hot gas with low density, thermalized by inverse wind shock. Young starbursts can contain the compact cavities inside HII region. Diffuse ionizing radiation, that arises in the cavity could considerably affect the medium ionization. Outside the stellar wind bubble a thin dense shell formed by the direct wind shock is located. This shell can appreciably transform the shape of the ionizing radiation spectrum in neighbouring region. We investigate this possibility, using the density and temperature distributions of density and temperature, and other physical parameters of bubble-like structures given by Weaver et al. (1977).

Key words: bubbles, evolution, HII regions

INTRODUCTION

We intend to use multicomponent photoionization modelling (PhM) for the studying of the influence of embedded bubbles in HII region surrounding starburst on the changing of the ionization spectrum shape. The first and second inner components of such modelling correspond to the hypersonic stellar wind zone and the region of shocked stellar wind respectively. The distributions of the gas density and temperature in these components are derived from the bubble structure obtained from equations of continuity and energy transfer, including thermal conductivity [4]. The third component is a thin shell of high density gas formed by the wind shock. The value of its density was obtained from isobaric condition at contact discontinuity between the second and third components. The fourth component is the ordinary HII region. Input spectrum of ionizing radiation was obtained from the starburst model for a wide range of ages and metallicity.

THE METHOD OF CALCULATIONS

The structure of the typical bubble is shown in Fig. 1), where “a” is the hypersonic stellar wind, “b” is the hot, almost isobaric region of shocked stellar wind, “c” is the thin, dense shell of interstellar gas, “d” is the typical HII region.

For our multicomponent photoionization modelling we used the following free parameters: age of nebula t (varied from 1 to 10 Myr), mass-loss of starburst \dot{M}_w (varied from 10^{-5} to $10^{-3} M_{\odot}/\text{year}$); velocity of stellar wind v_w (varied from 20 to 2000 km/s), and density of interstellar gas n_0 (varied from 1 to 1000 cm^{-3}).

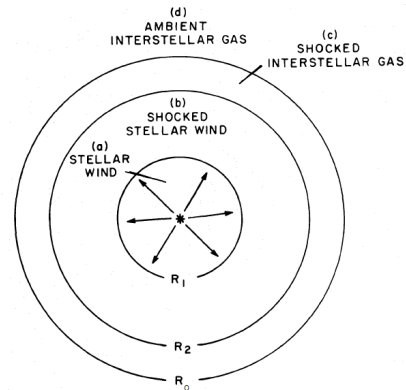


Fig. 1: Structure of the typical bubble.

We used the `Cloudy 08.00` code [1] for the photoionization modelling, and the `Starburst99` code [2] for calculation of the energy distribution in ionizing spectrum (the so-called Lyc-spectrum) from the starburst region. What is noteworthy, that each of Lyc-spectra from the starburst region was calculated at the corresponding model age. We modified the `Cloudy 08.00` code for the realization of the multicomponent photoionization modelling.

Physical conditions along the radius of the stellar wind bubble were determined as a solution of the following equations of continuity and energy transfer, taking into account the thermal conductivity [4]:

$$\frac{1}{\xi^2} \frac{d}{d\xi} (\xi^2 u) - \frac{u - \xi}{\tau} \frac{d\tau}{d\xi} = \frac{22}{21}, \quad (1)$$

$$\frac{1}{\xi^2} \frac{d}{d\xi} \left(\xi^2 \tau^{\frac{5}{2}} \frac{d\tau}{d\xi} \right) - \frac{3}{2} \frac{u - \xi}{\tau} \frac{d\tau}{d\xi} = \frac{13}{35}. \quad (2)$$

*ihorkoshmak@gmail.com

†bmelekh@gmail.com

The “b” shell has internal R_1 and external R_2 radii, respectively:

$$\begin{aligned} R_1 &= 5.7\dot{M}_6^{0.3}n_0^{-0.3}v_{2000}^{0.1}t_6^{0.4}[\text{pc}], \\ R_2 &= 27\dot{M}_6^{0.2}n_0^{-0.2}v_{2000}^{0.4}t_6^{0.6}[\text{pc}], \end{aligned} \quad (3)$$

where $\dot{M}_6 = \frac{\dot{M}_w}{10^{-6}}$, $v_{2000} = \frac{v_w}{2000}$, $t_6 = \frac{t}{10^6}$; τ and u are dimensionless variables which are functions only of a dimensionless radial coordinate $\xi = \frac{r}{R_2(t)}$.

The density of the third component n_s was obtained from the isobaric condition at contact discontinuity between the second and third components. We calculated thickness of the third component using the following expression [3]:

$$\Delta r = R_2 \left\{ \left(1 - \frac{n_0}{n_s} \right)^{-\frac{1}{3}} - 1 \right\} [\text{pc}]. \quad (4)$$

In our case, the electron temperature can be determined in two ways: (1) from the energy balance equation in photoionization modelling, and (2) from the hydrodynamic model of the bubble.

The first way was used to calculate of the electron temperature values in “c” and “d” components. But the temperature in “a” and “b” components was obtained using the second way, because in these cases it is defined mainly by hydrodynamic processes.

For our investigations we used the hydrodynamic model of the stellar wind bubble from [4]. Thus, the boundary conditions are the same as in [4]. The multicomponent model grid and its free parameters were obtained in accordance with the parameters of the bubble (mass-loss rate of the starburst, velocity of the stellar wind, age of the nebula). Thus, grid free parameters define the size of the bubble and physical conditions therein.

The radial distributions of gas density and temperature in the stellar wind bubble are given by the following approximate expressions:

$$n_H = \text{DF} \cdot 10^{A_n(R)}, \quad T_e = \text{TF} \cdot 10^{A_T(R)}, \quad (5)$$

where $\text{DF} = n_0^{\frac{19}{35}} \cdot (\dot{M}_6 \cdot v_{2000}^2)^{\frac{6}{35}} \cdot t_6^{-\frac{6}{35}}$, $\text{TF} = n_0^{\frac{2}{35}} \cdot (\dot{M}_6 \cdot v_{2000}^2)^{\frac{6}{35}} \cdot t_6^{-\frac{22}{35}}$, $A_n(R) = \log n_a(R)$ and $A_T(R) = \log T_b(R)$, $A_T(R) = \log T(R)$ are the approximate expressions obtained as fits of the results

from [4]:

$$\begin{aligned} \log n_a(R) &= -3.82495 + \\ &+ 1.00971e^{-\frac{R+0.17442}{0.25075}} + 2.5191e^{-\frac{R+0.17442}{1.94557}}, \\ \log n_b(R) &= 64.03901471 - 48.80541204 \cdot R + \\ &+ 13.97542937 \cdot R^2 - 2.11750182 \cdot R^3 + 0.18978405 \cdot R^4, \\ &- 0.01042102 \cdot R^5 + 3.44806684 \cdot R^6 - \\ &- 6.31658041 \cdot 10^{-6} \cdot R^7 + 4.9239613 \cdot 10^{-8} \cdot R^8, \end{aligned} \quad (6)$$

$$\begin{aligned} R &= 0.005 \div 6.205[\text{pc}]; \quad \log T_{fit1}(R) = 4.64; \\ R &= 6.205 \div 9.205[\text{pc}]; \quad \log T_{fit2}(R) = 5.84892 + \\ &+ 2.83179 \cdot (1 - e^{-\frac{R-6.11145}{0.25075}})^{0.49234} \cdot e^{-\frac{R-6.11145}{3.48938}}; \\ R &= 9.205 \div 22.505[\text{pc}]; \\ \log T_{fit3}(R) &= -6.429060955 + 6.299770486 \cdot R - \\ &- 1.157442226 \cdot R^2 + 0.10650819 \cdot R^3 - \\ &- 0.005318678 \cdot R^4 + 0.000138352 \cdot R^5 - 0.000001474 \cdot R^6; \\ R &= 22.505 \div 27[\text{pc}]; \\ \log T_{fit4}(R) &= -1912462.460571898 + \\ &+ 472743.449417495 \cdot R - 48663.85822284 \cdot R^2 \\ &+ 2670.237186899 \cdot R^3 - 82.372465048 \cdot R^4 + \\ &+ 1.354511416 \cdot R^5 - 0.009275676 \cdot R^6. \end{aligned} \quad (7)$$

Expressions (6) and (7) are obtained for typical bubble with $R_1=5.7$ pc and $R_2=27$ pc and were rescaled to the corresponding bubble size for each of the grid models (see Figs. 2, 3).

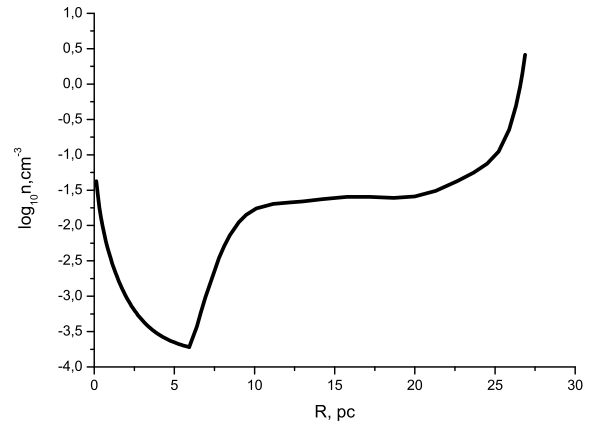


Fig. 2: Figure is based on approximation expression of distribution of density, (6).

Models of all components were calculated separately. But ionizing radiation propagates from the central starburst region in outward direction through

the bubble components. Thus, for an example, photoionization in “d” component is caused by ionizing photons with energy distributed differently than that in Lyc-spectrum calculated using the **Starburst99** code [2], because the shape of the photon energy distribution has been transformed in components it passed through. As it also was mentioned above, the density in third component was obtained from isobaric condition at contact discontinuity between the second and third components. Hence, the physical conditions in the third component depend on those in the second component.

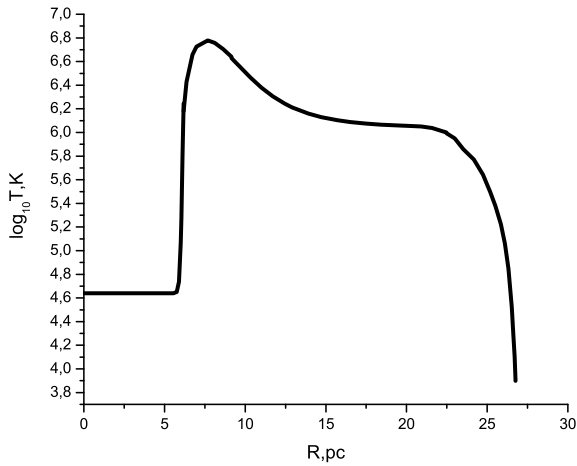


Fig. 3: Figure is based on approximation expression of distribution of temperature, (7).

RESULTS AND CONCLUSIONS

The evolution grid of multicomponent photoionization models with different bubble parameters was calculated. The contribution of the stellar wind bubble components to the changes of the energy distribution shape in ionizing spectrum (Lyc-spectrum) was analysed. We identified three types of this effect: without the lack of quanta beyond the Lyman limit (1 Ry) (Fig. 4), with the lack of quanta beyond the Lyman limit (this lack was formed by the third component) (Fig. 5), and partial case with the lack of quanta beyond the Lyman limit when bubble forms the excess of quanta (Fig. 6). The excess of quanta appears due to contribution of the second component that emits quanta excess beyond 5-6 Ry (comparing with the input Lyc-spectrum, calculated using **Starburst99** code [2]).

This excess mainly reveals in models with the age larger than 5 Myr. Such old bubbles should be very extended (hundreds of parsecs). Therefore at this age the excess is not caused by the stellar ionizing emission and the presence of massive O and B stars is not a necessary condition for its appearance.

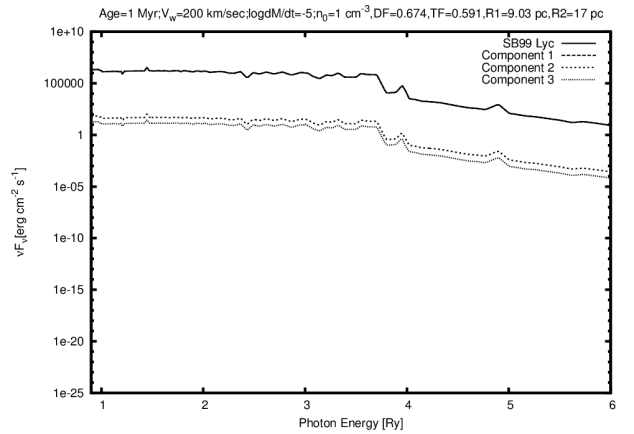


Fig. 4: Type without lack of quanta beyond Lyman-continuum limit.

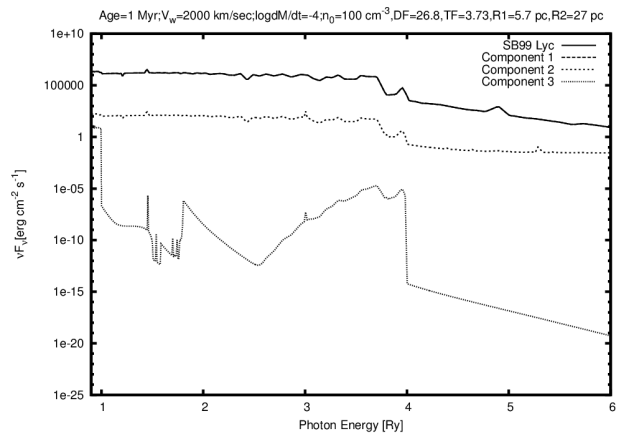


Fig. 5: Type with lack of quanta beyond Lyman-continuum limit (this lack was formed by third component).

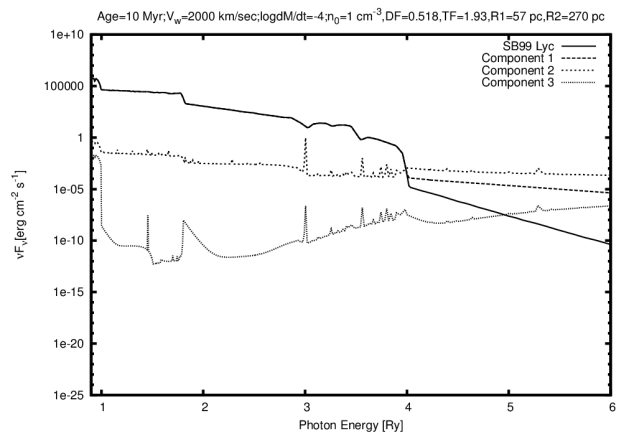


Fig. 6: Partial case with lack of quanta beyond Lyman-continuum limit when bubble forms the excess of quanta.

One can see that the gap in spectrum within en-

ergy range 1-4Ry arises in Ly α -spectra if photons propagate through the thin dense envelope. That is due to the fact that photons energy dependence of the cross section, σ_ν , for hydrogen-like ions has a peak at its ionization potential, and then rapidly decreases with increasing of the photons energy. In the case of high density envelope the free path of photons in environment with density n is defined as $l_\nu = 1/(\sigma_\nu n)$, hence photons with the energy close to the ionization potential will be absorbed, while those with higher energy will escape from such envelope.

ACKNOWLEDGEMENT

The research presented in this publication was supported by grant 0111U001087 of the Ukrainian National Foundation of Fundamental Researches.

REFERENCES

- [1] Ferland G. J. 2005, 'Hazy, A Brief Introduction to Cloudy 05.07, University of Kentucky Internal Report'
- [2] Leitherer C., Schaerer D., Goldader J.D. et al. 1999, ApJS, 123, 3
- [3] Vallee J. P. 1993, ApJ, 419, 670
- [4] Weaver R., McCray R., Castor J., Shapiro P. & Moore R. 1977, ApJ, 218, 377